Electrochemical Reversibility of Vinylferrocene Monolayers Covalently Attached on H-Terminated p-Si(100)

Franco Decker,[†] Fabrizio Cattaruzza,[‡] Carlo Coluzza,[§] Alberto Flamini,[‡] Andrea Giacomo Marrani,[†] Robertino Zanoni,[†] and Enrique A. Dalchiele*,[||]

Dipartimento di Chimica, Università degli Studi di Roma "La Sapienza", p.le A. Moro, 5-00185 Roma, Italy, CNR-ISM, Area della Ricerca di Montelibretti, C.P. 10, Monterotondo Stazione, 00016, Roma, Italy, Dipartimento di Fisica, Università degli Studi di Roma "La Sapienza", p.le A. Moro, 5-00185 Roma, Italy, and Instituto de Física, Facultad de Ingeniería, Herrera y Reissig 565, C.C. 30, 11000 Montevideo, Uruguay

Received: November 29, 2005; In Final Form: February 2, 2006

A reversible electrochemical behavior is demonstrated on a specially prepared redox-functionalized H−Si(100) surface, obtained via an extra-mild grafting procedure from vinylferrocene. The results of a detailed XPS and electrochemical characterization of the resulting hybrid are reported and discussed to propose it as a reference system for high-quality electroactive monolayers on Si. The investigated ferrocene derivative bears a functional group suitable for a mild route to covalent anchoring on Si, which is based on a photoinduced reaction with visible light under an inert atmosphere. Electrochemical reversibility is shown by sharp symmetric voltammograms on freshly prepared p-Si electrodes. Anodic oxide growth is responsible for the progressive degradation of the electrochemical response. Still, fast electron transfer to the surface redox species is maintained during several thousands cycles.

1. Introduction

Most electrochemical experiments performed so far with redox molecules attached on semiconductor surfaces have relied on the assumption that the electron-transfer mechanism is similar to that of a self-assembled monolayer (SAM) of redox centers on metal electrodes, as exemplified by ferrocene-terminated alkanethiol monolayers on Au.[1−3] However, the validity of this assumption, from the standpoint of electrochemical kinetics, requires that the semiconductor electrode is in a state of accumulation, with a half-filled band, during the charge-transfer process.[4] For redox couples such as $Fe(cp)_2^{0/+}$, reported to come only close to form an "ohmic" contact to p-Si,[5] the above assumption is questionable or may be valid only for the forward and not for the backward reaction. A second limitation to the above assumption might be set by the spatial self-organization of the molecules on a Si(100) surface, which could be less ideal than that of a SAM on a metal like Au. A good reason to choose the system vinyl-$Fe(cp)_2$ on Si(100) (VFC/Si) as a test bench was given in the literature,[6] where high-resolution STM images revealed linear arrangements of self-assembled vinyl-$Fe(cp)_2$ molecules on Si a few nanometers long. This is one of the very few known examples of a true molecular self-assembling on Si. The authors proposed, with the help of DFT calculations, that Si−C chemical anchoring occurs through the vinyl group with the ferrocene units forming a V-shaped, well-organized sequence on Si(100) to reduce the repulsive molecular interaction. Such an organized sequence of molecules on silicon would be greatly beneficial to the development of memory devices with a well-defined switching potential.

We present here results demonstrating that the system VFC/p-Si behaves electrochemically quite similarly to an ideal SAM on Au, although only under certain well-defined preparation conditions and during the first few voltammetric cycles. This behavior is experimentally represented by a characteristic voltammogram where the reduction wave, with the 90 mV fwhm predicted for an ideal noninteracting tethered group,[7] is the mirror image of the oxidation wave reflected across the potential axis. Important differences displayed by such monolayers grafted via wet chemistry on Si, when compared to SAMs on Au, are the residual reactivity of Si to ambient, which typically leads to hydrated suboxide or oxide layer growth, and the disorder of the redox centers when attached to a poorly defined Si surface. In previous publications about $Fe(cp)_2$ anchored on Si,[8−11] in fact, the voltammetric behavior reported was never as ideal as that of redox SAM's on gold. This lack of ideality may stem from several possible causes (the asymmetry of the redox reaction on a semiconductor electrode like p-Si, the variation in double-layer thickness during the reaction, or the inadequate self-assembly of the monolayer on Si implying the presence of an ensemble of redox centers in different environments). The above phenomena and the ion-pairing ability of the organic moiety with electrolyte ions or silanols surface groups have been discussed for electrodes treated electrochemically with multiple cv in light of XPS experiments and transient electrochemical techniques.

2. Experimental Section

The functionalization experiments on the surface-activated samples were carried out in a N_2(g)-purged drybox (MBraun) or using standard preparative Schlenk-line procedures.

Vinylferrocene was a Fluka pure reagent, used as received. All solvents used have been freshly distilled. Single-side polished Si(100) wafers (from Si-Mat), about 350 μm thick, p-doped (0.02 Ω cm resistivity) with areas of ca. 1 cm^2, were

* To whom correspondence should be addressed. Phone: ++598-2-7110905. Fax: ++598-2-7111630. E-mail: dalchiel@fing.edu.uy.
[†] Dipartimento di Chimica, Università degli Studi di Roma "La Sapienza".
[‡] CNR-ISM.
[§] Dipartimento di Fisica, Università degli Studi di Roma "La Sapienza".
[||] Instituto de Física, Herrera y Reissig 565.

10.1021/jp056921j CCC: $33.50
Published on Web 03/24/2006

first washed in boiling 1,1,2-trichlorethane for 10 min and subsequently in ethanol at room temperature with sonication for 5 min. Oxidation and further removal of residual organic impurities were carried out using the RCA1 procedure.[12] A solution of $H_2O/NH_4OH/H_2O_2$ (5:1:1) was prepared heating H_2O/NH_4OH (5:1) at 343 K, then adding H_2O_2, and boiling for 2 min. The silicon wafer was soaked in the hot solution for 15 min and then rinsed copiously with ultrapure deionized water (Water PLUS, Carlo Erba Reagents). Then residual metal ions were removed using the RCA2 procedure.[12] A solution of $H_2O/HCl/H_2O_2$ (6:1:1) was prepared heating H_2O/HCl (6:1) at 343 K, then adding H_2O_2, and boiling for 2 min. The silicon wafer, after the RCA1 cleaning, was soaked into the hot RCA2 solution for 10 min and then rinsed copiously with ultrapure deionized water. Then the clean oxidized wafer was etched with 10% aqueous HF for 10 min, rinsed with water again, dried under a stream of N_2, and immediately used in the functionalization process in a drybox.

Functionalized Si samples were prepared following the photoimmobilization route on freshly etched Si(100) substrates. H-terminated Si(100) wafer was placed in a leveled Petri dish inside the drybox, covered with VFC, and subjected for 1 h to a visible light irradiation from a quartz−iodine lamp (35 mW/cm^2) while being heated slightly above the melting point of VFC ($\geq$323 K).

After functionalization, all samples were subjected to the same cleaning procedure, consisting of four sonication cycles, 5 min each, with different solvents (CH_2Cl_2 and CH_3CN), and dried in a stream of N_2.

The RCA procedures have the advantage of leading to a total removal of the organic impurities from the surface and formation of a compact oxide layer, as revealed by a static contact angle of 0° with respect to water. On the other hand, the oxidation treatment leads to an increase of the surface roughness, as estimated with an atomic force microscope AFM (VT Omicron NanoTechnology), by the standard deviation from the average *z*-height value. AFM measurements on VFC/p-Si have shown a surface roughness of 0.15 nm, compatible with (sub)monolayer deposition.[10]

After monolayer formation ohmic contact was made to the back of the derivatized silicon samples scratching the Si surface, rubbing it with Ga−In eutectic, and attaching a copper contact to it. The electrode setup was obtained by pressing the Si crystal against an O-ring, sealing a small aperture in the PTFE cell, exactly defining the electrode area (0.3 cm^2).

The electrochemical properties of the ferrocene derivative monolayers covalently bound to p-Si(100) surfaces were first explored by cyclic voltammetry in 0.1 M NEt_4ClO_4 (tetraethylammonium perchlorate, TEAP) in dry CH_3CN. The electrolyte solution contained no deliberately added electroactive species. All electrochemical measurements were performed inside a drybox with a three-electrode cell using an Autolab Electrochemical Analyzer (model PGSTAT 12, Eco Chemie BV, The Netherlands). The counter electrode was a platinum coil wire, and a silver wire immersed in 0.01 M $AgNO_3$/0.1 M TEAP in CH_3CN, separated from the main solution by a porous fritted glass + agar plug, served as a reference electrode. All potentials reported will be henceforth referred to this reference. The kinetic analysis was performed after isolating the faradaic current from the charging current and after correcting the cyclic voltammograms for IR drop. Chronoamperometric measurements have been taken with the same electrochemical apparatus in two different ways: stepping the electrode potential from −0.3 to +0.3 V or higher (to record anodic transients) and on the step back from +0.4 to −0.3 V or lower (to record cathodic transients).

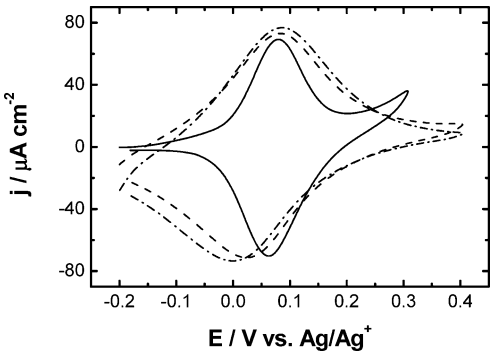

Figure 1. Cyclic voltammograms for a VFC/p-Si electrode in 0.1 M TEAP/CH_3CN: (—) first cycle and (- - -) after 10 and (— · —) 500 cyclic voltammetries aging. Scan rate: 1 V s^{-1}. Electrode area: 0.3 cm^2.

Experimental XPS. X-ray photoelectron spectroscopy (XPS) results have been obtained on an experimental apparatus in UHV consisting of a modified Omicron NanoTechnology MXPS system with an XPS chamber equipped with a monochromatic X-ray source (Omicron XM-1000) and an Omicron EA-127 energy analyzer. Samples were transferred between the various experimental areas by means of linear magnetic transfer rods or manipulators. All measurements have been conducted in the least possible time after sample preparation. Samples were produced and mounted on sample holders in a drybox, transferred from the drybox to the XPS facility in Schlenk tubes, under N_2, and introduced in the XPS chamber after about 1 min air exposure. No sizable sign of sample degradation under extended acquisition times under the X-rays was observed for the samples. The experimental conditions adopted were as follows: excitation by Al Kα photons ($h\nu$ = 1486.6 eV), generated operating the anode at 14−15 kV, 10−20 mA. No charging was experienced by the hybrid species as can be inferred from the Si 2p peak position, coincident with literature reports which assign a value of 99.7 eV to the Si $2p_{3/2}$ bulk component. XPS atomic ratios for the functionalized hybrids have been estimated from experimentally determined area ratios of the relevant core lines, corrected for the corresponding theoretical atomic cross-sections and for a square-root dependence of the photoelectrons kinetic energies. The effects on quantitative analysis possibly of photoelectron diffraction at preferential directions of electron collection[13] were minimized by mounting the Si(100) wafers always with the same orientation with respect to the analyzer axis. The sampling depth has been varied by collecting spectra at 11° and 61° with respect to the sample surface normal (sampling depth 2.37 nm at 11° and 1.17 nm at 61° according to ref 13).

3. Results

Cyclic Voltammetry and Chronoamperometry. The 1st, 10th, and 500th cyclic voltammograms (cv) of a p-Si(100) electrode functionalized with VFC in CH_3CN/TEAP (0.1 M) are shown in Figure 1. The electrode potential was scanned from the lower to higher limit and back at 1 V/s, inducing the reversible oxidation of $Fe(cp)_2$ derivative groups. The first cv scan profile shows very symmetric ferrocene oxidation and ferricenium reduction peaks with a full-width at half-maximum (ΔE_{fwhm}) of about 100 mV and with a 9 mV splitting between the anodic ($E_{p,a}$) and cathodic ($E_{p,c}$) peak potentials, $\Delta E_{p,p}$ ($\Delta E_{p,p} = E_{p,a} - E_{p,c}$). During the forward sweep (see the first

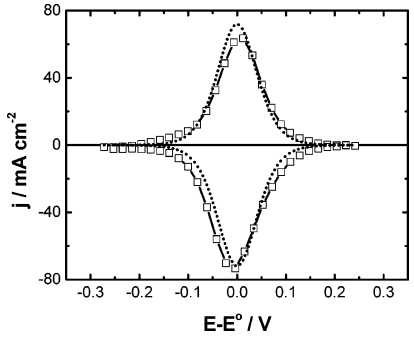

Figure 2. Experimental cyclic voltammogram of a VFC/p-Si electrode in 0.1 M TEAP/CH_3CN, after subtraction of the background (open squares), compared with the theoretical calculated response for an ideal Nernstian curve (see text) (dotted lines). $E°$ is the formal potential (73 mV). The experimental curve corresponds to the first one obtained in Figure 1. Scan rate: 1 V s^{-1}. Electrode area: 0.3 cm^2.

scan) an exponentially rising current at more positive potentials than the redox reaction has been observed. Moreover, a characteristic feature of the cv was the increase in the double-layer charging current when the VFC was fully oxidized. Smalley et al. found a similar behavior for ferrocene-terminated alkanethiol monolayers on gold.[2] The changes in the cv profile were the largest during the first 10 scans, whereas only limited changes were observed afterward. After 500 cycles aging there was no further change in the appearance of the cyclic voltammograms. This result demonstrates the stability of the modified VFC/p-Si electrode.[14] It is important to note that the position of the anodic peak potential remained fixed at almost the same value during the different aging cycles. This is an indication, from an energetic point of view, that the oxidation process for the VFC always requires the same energy. However, the cathodic peak shifted to a more negative potential as the number of cycles increased, indicating that the reduction process had become energetically less favorable.

Figure 2 shows the comparison of experimental and theoretical cyclic voltammograms. The solid curve is the cyclic voltammogram recorded for a VFC/p-Si electrode after an exponential background current has been subtracted. A formal potential of 73 mV, taken as the average of the peak potentials of the first scan reported in Figure 1, has been obtained. The area under the curve corresponds to about 8×10^{-11} mol cm^{-2} of VFC molecules attached to the p-Si(100) surface. Assuming that the VFC electrochemical reaction obeys the Nernst equation (in terms of surface concentrations), the ideal current−potential cyclic voltammogram curve should be according to[15]

$$i = -\frac{n^2F^2\Gamma_T\nu}{RT}\frac{\xi}{(1+\xi)^2} \qquad (1)$$

where Γ_T is the total amount of VFC attached onto the silicon surface, ν is the potential scan rate, $\xi = \exp[(nF/RT)(E - E^o)]$, E^o is the formal potential, and the other symbols have their usual meaning. The dashed curve in Figure 2 is the cyclic voltammogram calculated on the basis of eq 1, employing the value of Γ_T obtained from integration of the area under the experimental voltammogram (after background current subtraction). Application of eq 1 produces a good qualitative fitting, particularly satisfactory in the reverse cathodic semicycle where the same experimental and theoretical peak current can be appreciated.

Representative cyclic voltammograms for VFC/p-Si in CH_3CN/TEAP (0.1 M) at different scan rates, obtained after the 10th cv, are shown in Figure 3. The electrode potential was scanned

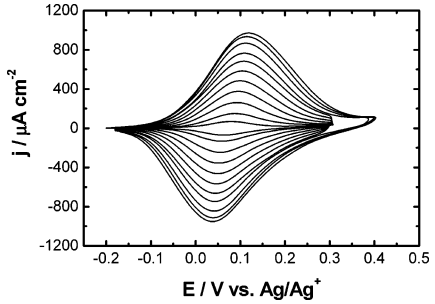

Figure 3. Representative cyclic voltammograms of a VFC/p-Si-functionalized electrode in 0.1 M TEAP/CH_3CN as a function of the potential scan rate. The scan rate values are from 1 to 11 V/s, from smallest to largest amplitude. Geometrical electrode area = 0.3 cm^2.

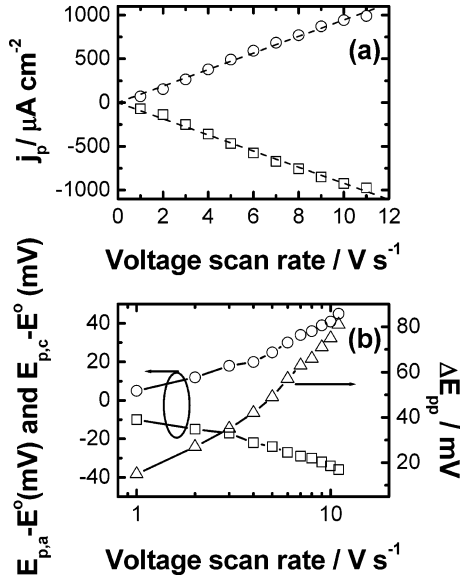

Figure 4. (a) Peak current density as a function of cv scan rate of VFC redox peaks derived from cyclic voltammetry of Figure 3: (○) anodic peak current density; (□) cathodic peak current density. (b) Influence of scan rate on VFC redox position and peak separation: (○) $E_{p,a}$, (□) $E_{p,c}$, (△) ΔE_{pp}).

from the lower to higher limit and back at scan rates varying from 1 to 11 V/s. As it can be inferred from inspection of Figure 4a, the anodic and cathodic peak currents were found to scale linearly with the scan rate υ rather than with $\upsilon^{1/2}$, indicating a surface redox process. This trend is characteristic of a reversible (Nernstian) electrochemical process wherein the relative activity of the ferrocene and ferricenium sites is uniform throughout the film and at equilibrium with each applied electrode potential.[16,17] As the scan rate increased, the separation between the anodic and cathodic peak potentials became larger, growing more rapidly on the side of the oxidation process (Figure 4b). Scan-rate dependence of the peak separation, if determined by the intrinsic charge-transfer rate to the ferrocene redox centers, can be used to evaluate the standard electron-transfer rate constant according to Laviron's approach.[10,18] With this approach, taking the peak-to-peak separation at various scan rates shown in Figure 4b, the average value of k_o was 130 s^{-1}. The electron-transfer rate constant has been evaluated by chronoamperometric experiments as well. In such experiments the slope of the ln i vs t curve at electrolysis times from 1 to 10 ms was evaluated to deduce the apparent rate constant k_{app} (the RC cell time constant being typically less than 1 ms) according to the procedure described in a previous work.[19] The semilogarithmic plot of the k_{app} values vs the final step potential is shown in Figure 5. From this plot, according to the classical Butler−

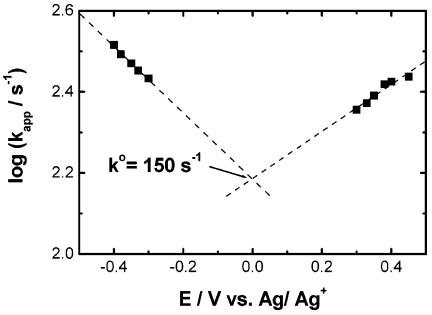

Figure 5. Representative semilogarithmic plot of the k_{app} values vs the final step potential for the VFC/p-Si system. The intercept of the anodic and cathodic branches yield $k° = 150\ s^{-1}$.

Volmer formalism, the standard rate constant k_o, evaluated from intercept of the straight lines fitting the measured k_{app} values, was 150 s^{-1}.

XPS Analysis. In recent reports[10,11] we made use of XPS to both assess the nature of the substrate−molecule interaction and establish the evolution of VFC on the Si surface upon electrochemical aging. The main conclusions coming from XPS were that a Si−C covalent bond is established between the two moieties, allowing for the stable presence of VFC upon thousands of redox cycles. These previous findings are confirmed by the present higher resolution XPS data, which allow for a more confident theoretical reconstruction of the peak envelopes for the freshly prepared VFC/p-Si, shown in Figure 6. The full photoelectron energy range only shows carbon-, silicon-, iron-, and oxygen-related peaks.

The C 1s line shape does not show any asymmetry toward the low-BE side. This is the energy region for the C−Si bond in fully saturated anchored alkyl monolayers.[20,21]

Such a component, however, is known to progressively shift toward the position characteristic for carbon atoms in an aromatic ring, along the sequence Si−C≡C, Si−C═C, Si−C−C. Moreover, the mechanism proposed for the photoinduced anchoring of a vinyl functional group on hydrogenated silicon suggests the establishment of a fully saturated (Si−)C−C bond sequence. Therefore, the present experimental lack of a C 1s component separated from the one associated to the cyclopentadienyl rings suggests that the vinyl group is saturated. The C/Fe XPS atomic ratio (12) is fully consistent with the molecular formula for the intact species if the whole Fe $2p_{3/2}$ energy region is taken into account.

Silicon. A typical Si 2p XPS spectrum from VFC/p-Si is reported in Figure 6a. Two spin−orbit split components result from curve fitting, respectively, related to bulk Si atoms, located at a binding energy (BE) of 99.7 eV, and a surface contribution, enhanced at grazing photoelectron collection angle, Figure 6b. The +0.34 eV BE shift of the latter with respect to the bulk component is consistent with literature reports on similar systems.[22]

Two main experimental findings are worth commenting: (a) No component can be located in the Si $2p_{3/2}$ spectrum at a BE

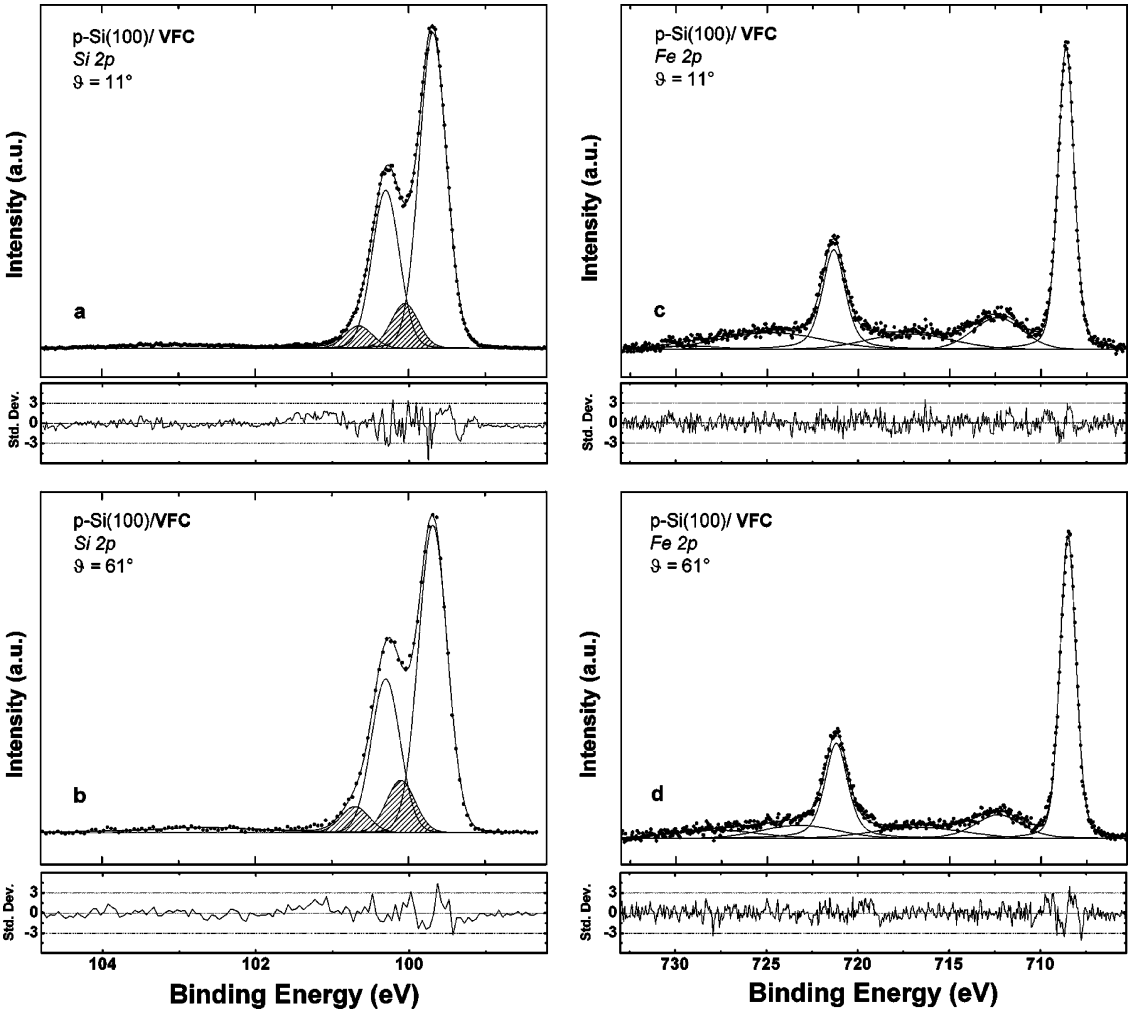

Figure 6. XPS spectra of freshly prepared VFC/p-Si taken from the Si 2p (left) and Fe 2p (right) regions, collected at 11° and 61° photoelectron collection angles. The corresponding residuals are plotted in standard deviation (σ) units.

lower than the bulk, which calls for a (nearly) defect-free surface;[10,22,23] (b) An oxide-free surface has been obtained, as clearly indicated by the flatness of the Si 2p BE energy region in the range typical for silica (103−104 eV). Both effects testify to the high quality of the functionalized surface. Photochemical anchoring clearly produces a surface well passivated by the attached molecules.

Iron. Fe species in both the II and III oxidation states have been, respectively, found at 708.6 and 712.2 eV BEs, Fe(II) being largely predominant. Curve fitting of the complex Fe 2p peak envelopes has been applied to separate Fe(II) and Fe(III) data sets. The corresponding BE and fwhm values reproduce literature findings for pure and surface-reacted ferrocene and ferricenium salts, respectively.[24,25] The narrow fwhm of Fe(II) spectra for VFC/p-Si favors an assignment to a well-defined surface species. As for the Fe(III) species, a possible assignment to Fe_2O_3, which has been sometimes reported in surface-anchored ferrocenes,[26] can be confidently excluded on the basis of the main peak-to-satellite Fe $2p_{3/2}$ energy separation and the relative intensity of Fe $2p_{3/2}$ satellite to main lines in Fe_2O_3.[25] This assignment is also consistent with the C/Fe atomic ratio, discussed above. The Fe(II)/Fe(III) atomic ratios, determined from the corresponding intensity of the Fe $2p_{3/2}$ component at 11° and 61°, are strictly comparable, as clearly visible in Figure 6. The lack of surface enrichment in one of the Fe components can be taken as further direct evidence for the proposed assignment of Fe(II) and Fe(III) species to substituted ferrocene and ferricenium both directly bound to silicon.

4. Discussion

The symmetrical shape of the first cv of the vinyl-$Fe(cp)_2$ covalently attached to Si can be seen as direct proof of a reversible charge-transfer process which, in turn, also testifies for the high quality of the grafted redox monolayer, prepared along the described procedure. In fact, the small associated $\Delta E_{p,p}$ indicates that the electron transfer rate across the monolayer is initially fast compared to the 1 V/s scan rate; moreover, the observed value of ≈100 mV for ΔE_{fwhm} agrees fairly with the 90 mV predicted (and entropically determined) for ΔE_{fwhm} with an ideal noninteracting tethered redox group at room temperature.[27] The above voltammetric characteristics would suggest that the ferrocene groups on a freshly prepared p-Si are nearly identical and that they lie outside the interfacial charge double layer because otherwise a much broader and shifted peak would be expected.[28] The small difference between the calculated and observed curves in Figure 2 can be attributed to the fact that the surface activities of the attached molecules differ from their surface concentrations, as shown by Brown and Anson.[15] In the present work, the very poor surface stability to oxidation of the Si electrode functionalized with a redox monolayer did not allow us to deduce meaningful interaction parameters as for a derivatized noble metal electrode. We interpreted the rapid evolution with time of the electrochemical behavior of this SAM on Si as being due to the growth of a partially passive oxide or suboxide on the nonderivatized Si surface sites. In fact, the exponentially rising background current on the positive potential sweep decreased after a few cycles, as expected for a passivation reaction, and the analysis of the Si 2p XPS spectrum has consistently shown an increase of the oxide peak after cyclic voltammetry.[11] Oxide growth also explains the rapid increase of ΔE_{fwhm} and the associated more progressive one of $\Delta E_{p,p}$ observed during the first 500 scans. Experimental values of ΔE_{fwhm} exceeding the theoretical values have been attributed to the existence of multiple formal potentials, which in turn implies the presence of an ensemble of redox centers in different environments, with a negligible rate of conversion between environments within the monolayer. This is the case for a monolayer with redox centers lying both on the outer surface and inside a thin insulating oxide-like domain, an occurrence related to the very short length of the organic chains attached to our p-Si samples. It has also been speculated that wave broadening may be the result of variations of the double-layer thickness[28] and of the surface charge taking place during faradic reactions involving the attached electroactive centers, resulting in fluctuations of the surface potential.[29]

The progressive negative shift of the formal redox potential of the ferrocene groups in the monolayer can be associated to the interaction of ferrocene/ferricenium moieties with the progressively increasing modification of the local environment. A gradual stabilization of the ferricenium ion in the oxide environment growing around the redox centers can be put forward, likely accompanied by ion pairing of Fe(III) with anions[30] (ClO_4^- from the electrolyte or O^- sites from deprotonated silanol terminations). As we discussed elsewhere,[10] this stabilization of the ferricenium ion has been deduced by the decrease of the Fe(II)/Fe(III) ratio due to aging under cv, as measured by XPS spectra in the Fe 2p region. However, the absence of Cl signals in such spectra strongly suggests that ion pairing of Fe(III) with O^- sites is the prevailing mechanism.

The increase in $\Delta E_{p,p}$ for the VFC/p-Si system after the 10th cycle was analyzed as a function of scan rate. At sufficiently low scan rates the observed $\Delta E_{p,p}$ was only ca. 15 mV even after tens of cv's, i.e., only slightly higher than the value of 0 mV expected for surface-bound species. This deviation from ideality may be partly due to voltage drops in the system.[31] As the scan rate increased, however, $E_{p,a}$ moved to more anodic values at a higher rate than $E_{p,c}$ to more cathodic ones. The low values of the rate constant k_0 (130−150 s^{-1}) calculated from cv and chronoamperometry indicated inhibition of the electron transfer from redox centers at the partially oxidized Si surface. The reaction asymmetry suggested that the oxidation and reductions steps encounter different kinetic limitations, perhaps due to a slight asymmetry of the energy barrier for the electron-transfer process. The presence of an asymmetric energy barrier was confirmed by the different slopes of the respective branches in the Tafel plot of Figure 5, indicating different anodic and cathodic transfer coefficients (α_a and α_c, respectively). These transfer coefficients can be extracted from Figure 5, and α_a and α_c values of 0.9 and 0.1 have been obtained, showing that the anodic transfer is typically much higher than the cathodic one. An explanation reported for ferrocene SAMs on metals is that the reaction could follow a "square scheme" in which the reduction step does not follow the exact reverse path of the oxidation.[32] Moreover, it is evident that the anodic and cathodic processes are not the simple forward and backward reactions; perhaps interactions between Fe^{3+} and O^- cause a chemical complication and would be responsible for the reaction asymmetry. In a semiconductor electrode−redox system, as VFC/p-Si, another suitable explanation for this behavior can be a different rate of hole injection/extraction between the valence band and the redox head of the organic moiety as a function of the forward or reverse bias applied to the electrode. Hole injection in p-Si (during Fe(III) reduction) would be in principle favored because of the high density of valence-band states facing under reverse bias the redox level of the attached molecules. The injection of both a hot and thermal hole can account for the higher rate of the cathodic process.

5. Conclusions

We demonstrated that the electrochemical response of VFC molecules on p-Si(100) is that of an ideal, self-assembled monolayer as long as the Si substrate is oxide free. The highly reversible behavior of the redox monolayer on silicon would better define the switching potential of the hybrid electronic prototype device, thus being greatly beneficial to the ongoing development of molecular memories. The reversibility of the redox reaction is shown by the sharpness and symmetry of the peaks in the cv and confirmed by the good qualitative fitting with the equation describing an electroactive Nernstian behavior. The departure from this ideal voltammetric diagnostic was progressive with the electrochemical treatment and revealed a changing environment about the redox centers that was attributed to the Si anodic oxidation with a passivating effect. The redox kinetics, measured by cv at various scan rates and by chronoamperometry, was evaluated on electrodes already oxidized, indicating partial inhibition of electron transfer and the existence of an asymmetric energy barrier. Both the inhibition of redox kinetics and the apparent cathodic shift of the formal potential could be due to ion pairing of Fe(III) with surface groups occurring in the presence of an oxide layer with thickness comparable to that of the attached redox molecules.

Acknowledgment. The work has been supported by MIUR (Ministero dell'Istruzione, Università e Ricerca) through PRIN National Programs and the Università degli Studi di Roma "La Sapienza". E.A.D. carried out this work with the support of the ICTP Programme for Research and Training in Italian Laboratories (Associate Member), Trieste, Italy, which is kindly acknowledged.

References and Notes

(1) Rowe, G. K.; Creager, S. E. *Langmuir* **1991**, *7*, 2307.
(2) Smalley, J. F.; Feldberg, S. W.; Chidsey, C. E. D.; Linford, M. R.; Newton, M. D.; Liu, Y.-P. *J. Phys. Chem.* **1995**, *99*, 13141.
(3) Sumner, J. J.; Creager, S. E. *J. Phys. Chem. B* **2001**, *105*, 8739.
(4) Tan, M. X.; Lewis, N. S. *Inorg. Chim. Acta* **1996**, *242*, 311.
(5) Bocarsly, A. B.; Bookbinder, D. C.; Dominey, R. N.; Lewis, N. S.; Wrighton, M. S. *J. Am. Chem. Soc.* **1980**, *102*, 3683.
(6) Kruse, P.; Johnson, E. R.; DiLabio, G. A.; Wolkow, R. A. *NanoLett.* **2002**, *2*, 807.
(7) Bard, A. J.; Faulkner, L. R. *Electrochemical Methods*; John Wiley & Sons: New York, 1980; p 522.
(8) Li, Q.; Mathur, G.; Homsi, M.; Surthi, S.; Misra, V.; Malinovskii, V.; Schweikart, K.-H.; Yu, L.; Lindsey, J. S.; Liu, Z.; Dabke, R. B.; Yasseri, A.; Bocian, D. F.; Kuhr, W. G. *Appl. Phys. Lett.* **2002**, *81*, 1494.
(9) Roth, K. M.; Yasseri, A. A.; Liu, Z.; Dabke, R. B.; Malinovskii, V.; Schweikart, K.-H.; Yu, L.; Tiznado, H.; Zaera, F.; Lindsey, J. S.; Kuhr, W. G.; Bocian, D. F. *J. Am. Chem. Soc.* **2003**, *125*, 505.
(10) Zanoni, R.; Cattaruzza, F.; Coluzza, C.; Dalchiele, E. A.; Decker, F.; Di Santo, G.; Flamini, A.; Funari, L.; Marrani, A. G. *Surf. Sci.* **2005**, *575*, 260.
(11) Dalchiele, E. A.; Aurora, A.; Bernardini, G.; Cattaruzza, F.; Flamini, A.; Pallavicini, P.; Zanoni, R.; Decker, F. *J. Electroanal. Chem.* **2005**, *579*, 133.
(12) In *Handbook of Semiconductor Cleaning Technology*; Kern, W., Ed.; Noyes Publishing: Park Ridge, NJ, 1993; Chapter 1.
(13) Seah, M. P.; Spencer, S. *J. Surf. Interface Anal.* **2002**, *33*, 640.
(14) Cleland, G.; Horrocks, B. R.; Houlton, A. J. *Chem. Soc., Faraday Tans.* **1995**, *91*, 4001.
(15) Brown, A. P.; Anson, F. C. *Anal. Chem.* **1977**, *49*, 1589.
(16) Daum, P.; Murray, R. W. *J. Electroanal. Chem.* **1979**, *103*, 289.
(17) Han, L. M.; Rajeshwar, K.; Timmons, R. B. *Langmuir* **1997**, *13*, 289.
(18) Laviron, E. *J. Electroanal. Chem.* **1979**, *101*, 19.
(19) Foster, R. J.; Faulkner, L. R. *J. Am. Chem. Soc.* **1994**, *116*, 5444.
(20) Scandurra, A.; Renna, L.; Cerofolini, G.; Pignataro, S. *Surf. Interface Anal.* **2002**, *34*, 777.
(21) Wallart, X.; Henry de Villeneuve, C.; Allongue, P. *J. Am. Chem. Soc.* **2005**, *127*, 7871.
(22) Webb, L. J.; Nemanick, E. J.; Biteen, J. S.; Knapp, D. W.; Michalak, D. J.; Traub, M. C.; Chan, A. S. Y.; Brunschwig, B. S.; Lewis, N. S. *J. Phys. Chem. B* **2005**, *109*, 3930.
(23) Cerofolini, G. F.; Galati, C.; Renna, L. *Surf. Interface Anal.* **2003**, *35*, 968.
(24) Briggs, D.; Seah, M. P. *Practical Surface Analysis*, 2nd ed.; J. Wiley & Sons: Chichester, 1990; Vol. 1.
(25) Woodbridge, C. M.; Pugmuir, D. L.; Johnson, R. C.; Boag, N. M.; Langell, M. A. *J. Phys. Chem. B* **2000**, *104*, 3085.
(26) Cowan, D. O.; Park, J. *Chem. Commun.* **1971**, 1444.
(27) Finklea, H. O. In *Encyclopedia of Analytical Chemistry*; Meyers, R. A., Ed.; John Wiley and Sons Ltd.: Chichester, 2000; pp 1−26.
(28) Smith, C. P.; White, H. S. *Anal. Chem.* **1992**, *64*, 2398.
(29) Sabapathy, R. C.; Bhattacharyya, S.; Leavy, M. C.; Cleland, W. E., Jr.; Hussey, C. L. *Langmuir* **1998**, *14*, 124.
(30) Ju, H.; Leech, D. *Phys. Chem. Chem. Phys.* **1999**, *1*, 1549.
(31) Zhao, Q. *Nanotechnology* **2005**, *16*, 257.
(32) Cruañes, M. T.; Drickamer, H. G.; Faulkner, L. R. *Langmuir* **1995**, *11*, 4089.